GNSS-BASED SIGNAL PATH DELAY AND GEODYNAMIC CORRECTIONS FOR CENTIMETER LEVEL PIXEL LOCALIZATION WITH TERRASAR-X

Ulrich Balss[1], Christoph Gisinger[2], Xiao Ying Cong[3], Michael Eineder[1, 3], Thomas Fritz[1], Helko Breit[1], Ramon Brcic[1]

[1]*Remote Sensing Technology Institute (IMF), German Aerospace Center (DLR), Muenchner Strasse 20, D-82234 Oberpfaffenhofen, Germany, (ulrich.balss, michael.eineder, thomas.fritz, helko.breit, ramon.brcic)@dlr.de*
[2]*Institute for Astronomical and Physical Geodesy (IAPG), Technische Universität München (TUM), Arcisstrasse 21, D-80333 Munich, Germany, christoph.gisinger@bv.tu-muenchen.de*
[3]*Remote Sensing Technology (LMF), Technische Universität München (TUM), Arcisstrasse 21, D-80333 Munich, Germany, xiao.cong@dlr.de*

ABSTRACT

Previous studies have shown the unprecedented absolute pixel localization accuracy of the German SAR (Synthetic Aperture Radar) satellites TerraSAR-X and TanDEM-X. Now, by thoroughly correcting the atmospheric signal path delays and geodynamic effects like tides, loadings and plate movements, range accuracies of about 1 centimeter are demonstrated to be attainable. While Global Navigation Satellite System (GNSS) data provide local correction values for the atmospheric delays, correction values for the geodynamic effects are based on the IERS (International Earth Rotation and Reference Systems Service) conventions. In order to verify the proposed correction approach, we set-up a long-term measurement series based on a corner reflector with very precisely known ground position which we installed at the Geodetic Observatory at Wettzell, Germany, close to the local GNSS reference site. Measurement series of further comparable high precision corner reflectors in Antarctica and Finland are in progress and shall prove the worldwide reproducibility of the achieved results.

1 Introduction

Spaceborne SAR (Synthetic Aperture Radar) is known for its ability to provide weather and time of day independent observation of the earth's surface and measurement of relative shifts based on the carrier phase (SAR interferometry). In contrast, our objective is the absolute pixel localization of a SAR image. Previous studies revealed the unprecedented localization accuracy of TerraSAR-X (TSX-1) and TanDEM-X (TDX-1) at the centimeter level [1-4]. Among others, this accuracy results from precise orbit determination [5] and from the elimination of several SAR processor approximations, in particular the so-called stop go approximation. However, as these aspects solely refer to the generation of SAR products, the image user need not care about them. In contrast, a discerning user has to thoroughly correct his measurements for all signal path delays and geodynamic effects when aiming at the centimeter level [6]. As these effects are likewise relevant for the Global Navigation Satellite System (GNSS), GNSS and the International GNSS Service (IGS) provide a primary data source for the respective correction values [7][8].

2 Measurement Method

Radar systems indirectly measure geometric distances by means of the two-way travel time of radar pulses from the radar transmitter to the ground and back to the radar receiver. In a focused SAR image, the instant of closest approach of the sensor and a target as well as the signal travel time at this instant define the two radar time coordinates of azimuth and range. Strictly speaking, a radar pulse has to be transmitted slightly before the instant of closest approach to be received slightly after this instant and the satellite moved meanwhile which causes a slight increase of the measured range time [2]. But this geometric effect is already compensated for in the TerraSAR-X Multimode SAR Processor (TMSP). Usually, the conversion from range time to geometric distance refers to the vacuum velocity of light. However, electrons in

the ionosphere as well as dry air and water vapor mainly contained in the troposphere introduce additional signal delays which have to be taken into account. In addition, geodynamic effects like tides, loadings and plate movements shift the true position of a ground target.
In order to verify the pixel localization accuracy of a SAR system, the range and azimuth times of corner reflectors in focused SAR images are corrected for the estimated propagation delays and compared with their reference values obtained from precise geodetic survey of their geometric phase center. The conversion of the spatial geodetic coordinates into expected radar times is based on the zero Doppler equations [9] and interpolation of the satellite's position.
Our recent measurement series is based on a 1.5 meter trihedral corner reflector which we installed at the Geodetic Observatory at Wettzell, Germany. In this way, we benefit from the very close distance (about 240 meters) to the local GNSS reference stations. The corner reflector was integrated into the reference station's local tie by terrestrial geodetic survey and therefore its coordinates in ITF2008 [10] are known very precisely (<1 centimeter).

3 Path Delay Corrections

Regarding the impact of the atmosphere on the observed ranges, SAR and GNSS measurements behave very similarly as both make use of radio signals in the Gigahertz range and thus, the concept of separating the atmospheric delay into a non-dispersive part (usually called tropospheric delay – even if it encloses also contributions from other atmosphere layers) and a dispersive part (ionospheric delay) which is well-established in the field of GNSS [11] can be adopted to SAR. Moreover, this allows a straight forward transfer of tropospheric and ionospheric signals that are observed by GNSS in terms of Zenith Path Delay (ZPD) and vertical Total Electron Content (vTEC) to the TerraSAR-X range measurements. Since Wettzell station is part of the global IGS GNSS network, all IGS products including the ZPDs and the daily Differential Code Biases (DCBs), which are required for the vTEC computation, are directly available for the individual Wettzell GNSS receivers [8]. The following two procedures were carried out for all Wettzell GNSS receivers available during the datatakes. Averaging over the receivers led to the individual tropospheric and ionospheric corrections for the corner reflector measurements.
In order to determine the actual tropospheric corrections, three steps are involved: first, the ZPDs, comprising the total impact of the troposphere, are divided into their hydrostatic and wet components by modeling the hydrostatic part with the equation of Saastamoinen [12]. Next, the two components are individually transferred from the height of the GNSS receivers to the height of the corner reflector using the procedure given in [13]. Finally, the Vienna Mapping Function 1 [13][14] is used to convert both ZPD components into the SAR acquisition geometry.
Like the tropospheric corrections, the corrections for the ionosphere are solely based on local GNSS measurements. When combined with the ionospheric Single Layer Model (SLM), the description of the ionosphere in terms of vTEC can be obtained from the geometry-free linear combination of dual-frequency GNSS measurements. This computation is possible for every measurement epoch since the usually unknown DCBs are provided by IGS for both the Wettzell receivers and all GNSS satellites. Thus, one obtains the vTEC as a sampled function of time at the Ionospheric Pierce Point (IPP, i.e. the point at which the line of sight intersects with the shell of the SLM) location of the GNSS satellites. By performing a least squares fit of a plane to the sparse GNSS-based vTEC distribution and interpolating the vTEC at the TerraSAR-X IPP, the ionospheric correction for the corner reflector observation can be calculated. The details of the whole procedure can be found in [15].
In contrast to GNSS, the orbits of TSX-1 and TDX-1 are still within the upper ionosphere and for this reason the upper portion of the ionosphere contributes to the GNSS based measurement values but not to the path delay of the radar signal. At present, we consider this fact by applying a 75% weighting factor [6]. A concept to separate both parts of the ionospheric delay, below and above the satellite, based on real measurements of the latter one by the satellite's GNSS receiver is subject of ongoing investigations.

4 Geodynamic Corrections

The most prominent geodynamic effects are solid earth tides and continental drift which cause a shift of up to a few decimeters over the course of a day or years, respectively. We already considered both effects in our previous investigations [1][2][6]. However, to obtain millimeter localization accuracy, smaller geophysical effects must also be compensated for: Atmospheric pressure loading and ocean tidal loading weigh on the tectonic plate. Their variation shifts the target position by several millimeters each. Pole tides are a secondary effect of the precession of the earth axis, and vary also at the millimeter level. Even weaker effects (tenths of a millimeter) are caused by ocean pole tides and atmospheric tidal loading.
All of these effects are estimated by state of the art models [16] and transferred to the TerraSAR-X acquisition geometry [1]. The correction of almost all of these effects follows the conventions issued by IERS (International Earth Rotation and Reference Systems Service) 2010 edition [16]. The only exception is atmospheric pressure loading that is not yet included in the IERS conventions but still in debate. Estimates of

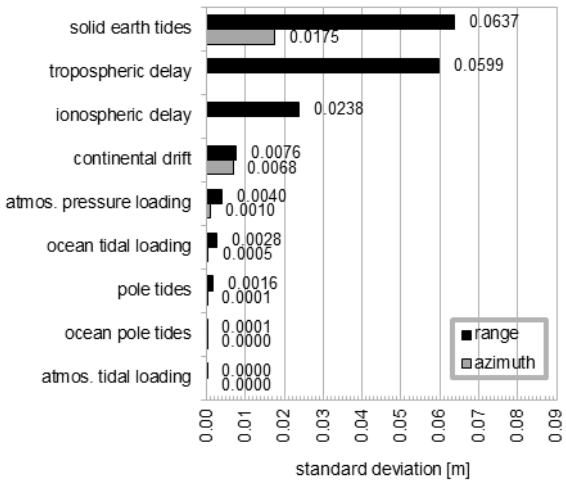

Figure 1: Standard deviations of geodynamic effects and signal propagation delays

this effect for a wide range of GNSS reference stations are available from the NASA atmospheric pressure loading service [17][18].

Figure 1 illustrates the proportions of the standard deviations of the individual geodynamic effects and signal propagation delays based on the example of our Wettzell measurement series. However, the amount of some effects may differ significantly from test site to test site, e.g. ocean tidal loading becomes more relevant for coastal test sites than for an inner land test site like Wettzell.

5 Measurement Results

Up to now, our Wettzell measurement series [7] consists of 35 TSX-1 and 6 TDX-1 datatakes which were recorded between July 12, 2011 and June 15, 2013. In case of one TSX-1 and two TDX-1 datatakes in winter 2012/13, a loss in radar cross section (RCS) of more than 10 dB (compared to the theoretically derived expected value which is actually reached in the other datatakes) indicates that there was a large amount of snow in the corner reflector which affected the validity of the respective position measurement. For this reason, we have to exclude these 3 datatakes from the analysis below.

Figure 2 shows the difference between measured and expected radar times after correcting the measured radar times for the signal propagation delays and the geodynamic effects (for convenience the time differences are converted to corresponding spatial distances). The major component of the observed range bias of -37.5 centimeters results from the instrument calibration constants which were determined based on a simplified model for the signal path delays [19] and therefore also contain atmospheric information. This calibration approach suffices for a localization accuracy better than 1 meter as specified in the TerraSAR-X product requirements [20]. In contrast, for high

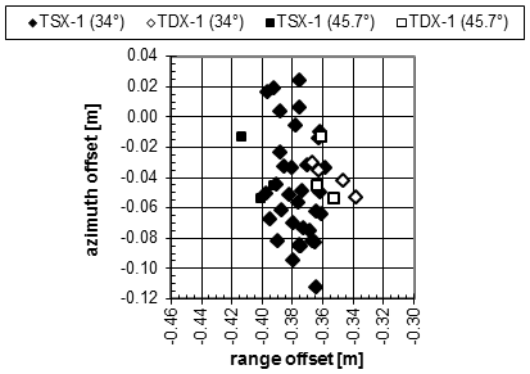

Figure 2: Difference between SAR and GNSS coordinates in radar geometry

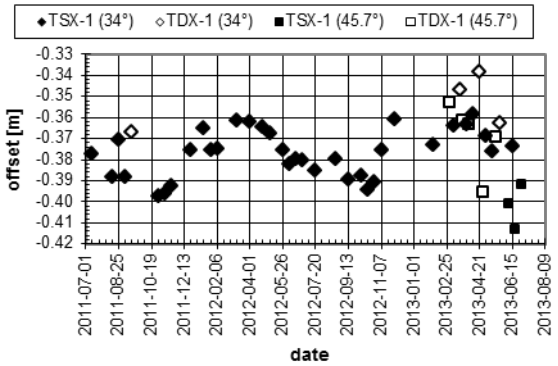

Figure 3: Temporal progression of the range offset

precision localizations an adaptation of the calibration constants is necessary. In the case of the TSX-1 repeat pass datatakes, the standard deviation of the differences amounts to 35.7 millimeters in azimuth and 11.2 millimeters in range. Based on the sparse statistics of the up to now acquired TDX-1 datatakes, the standard deviation for this satellite amounts to 9.8 millimeters in azimuth and 13.3 millimeters in range.

However, there is a strong temporal correlation between the measured range localizations as evident in **Figure 3**. A visual inspection of the temporal progression reveals that a good portion of the standard deviation results from a slow variation. In contrast, almost all immediately neighboring measurement values differ by millimeters for datatakes acquired by the same sensor. Thus, on a short-term scale, the measurements suggest that the localization accuracy for TSX-1 and TDX-1 could be further improved.

In order to investigate possible angular dependencies of the measured position offsets, we started a second measurement series with moderately different incidence angle (45.7 instead of 34 degree) at March 2, 2013. As any change in the orientation of the corner reflector would affect the precisely measured geodetic coordinates of its phase center, we left the reflector unchanged and accept a slight RCS reduction by about 2 dB. Based on the limited number of 7 up to now recorded datatakes, a first analysis reveals that there is at least no coarse localization offset against the results of the initial 34 degree measurement series.

6 Conclusions and Outlook

Both current measurement series will be continued. Major topics in the next stage of our project are the investigation of the angular dependency of our corrections and the worldwide reproducibility of the achieved performance. This will be analyzed by the setup of comparable high precision test sites throughout the world – two 1 meter trihedral corner reflectors were recently installed near DLR's GARS O'Higgins receiving station on the Antarctic Peninsula. The acquisition of datatakes from this test site started at March, 27, 2013. The setup of another test site with one corner reflector near the GNSS reference station Metsähovi, Finland, is in progress. In the long term, the geometric calibration of SAR sensors and the annotated corrections of SAR products will substantially benefit from the investigated correction schemes.

7 Acknownledgments

The work was partially funded by the German Helmholtz Association HGF through its DLR@Uni Munich Aerospace project "Hochauflösende geodätische Erdbeobachtung". We thank the Federal Agency for Cartography and Geodesy (BKG) for their kind allowance to install the corner reflectors at their Geodetic Observatory in Wettzell and for their local support. We thank our colleagues from DLR's Remote Sensing Data Center (DFD) who installed and maintain the corner reflectors at GARS O'Higgins.

References

[1] Eineder, M., Minet, C., Steigenberger, P., Cong, X.Y., Fritz, T.: *Imaging Geodesy – Toward Centimeter-Level Ranging Accuracy with TerraSAR-X.* IEEE Trans. on Geosci. and Remote Sens., Vol. 49, No. 2, 2011, pp. 661–671

[2] Balss, U., Eineder, M., Fritz, T., Breit, H., Minet, C.: *Techniques for High Accuracy Relative and Absolute Localization of TerraSAR-X / TanDEM-X Data.* Proc. IGARSS 2011, Vancouver, 2011, pp. 2464–2467

[3] Schubert, A., Jehle, M., Small, D., Meier, E.: *Mitigation of Atmosphere Perturbations and Solid Earth Movements in a TerraSAR-X Time-Series.* Journal of Geodesy, Online First, 2011

[4] Schubert, A., Small, D., Jehle, M., Meier, E.: *COSMO-SkyMed, TerraSAR-X, and RADARSAT-2 Geolocation Accuracy after Compensation for Earth-System Effects.* Proc. IGARSS 2012, Munich, 2012, pp. 3301–3304

[5] Yoon, Y., Eineder, M., Yague-Martinez, N., Montenbruck, O.: *Precise Trajectory Estimation and Quality Assessment,* IEEE Trans. on Geosci. and Remote Sens., Vol. 47, No. 6, 2009, pp. 1859–1868

[6] Balss, U., Cong, X.Y., Brcic, R., Rexer, M., Minet, C., Breit, H., Eineder, M., Fritz, T.: *High Precision Measurement on the Absolute Localization Accuracy of TerraSAR-X.* Proc. IGARSS 2012, Munich, 2012, pp. 1625–1628

[7] Balss, U., Gisinger, C. Cong, X.Y., Brcic, R., Steigenberger, P., Eineder, M., Pail, R., Hugentobler, U.: *High Resolution Geodetic Earth Observation: Correction Schemes and Validation.* Proc. IGARSS 2013, (to be published)

[8] Meindl, M., Dach, R., Jean, Y. (eds.): *International GNSS Service Technical Report 2011.* Astronom. Institute Univ. of Bern, 2012

[9] Cumming, I. G., Wong, F.H.: *Digital Processing of Synthetic Aperture Radar Data: Algorithms and Implementation.* , Boston, MA: Artech House, 2005, Ch. 4.2–4.3, pp. 114–129

[10] Altamimi, Z., Collilieux, X., Métivier, L.: *ITRF2008: An Improved Solution of the International Terrestrial Reference Frame,* Journal of Geodesy, Vol. 85, No. 8, 2011, pp 457–473

[11] Hofmann-Wellenhof, B., Lichtenegger, H., Wasle, E.: *GNSS Global Navigation Satellite Systems.* Wien, New York: Springer, 2008

[12] Saastamoinen, J.: *Contributions to the Theory of Atmospheric Refraction Part II. Refraction Corrections in Satellite Geodesy.* Bulletin Géodésique, Vol. 107, No. 1, 1973, pp. 13–34

[13] Kouba, J.: *Implementation and Testing of the Gridded Vienna Mapping Function 1 (VMF1).* Journal of Geodesy, Vol. 82, No. 4–5, 2007, pp. 193–205

[14] Boehm, J., Schuh, H.: *Vienna Mapping Functions in VLBI Analyses.* Geophys. Res. Lett., 31, L01603, DOI: 10.1029/2003GL018984, 2004

[15] Gisinger, C.: *Atmospheric Corrections for TerraSAR-X Derived from GNSS Observations.* master thesis, TU Munich, 2012

[16] Petit, G., Luzum, B. (eds.): *IERS Conventions (2010).* IERS Technical Note 36, Frankfurt: Verlag des Bundesamtes für Kartographie und Geodäsie, 2010, Ch. 7, pp. 99–122

[17] Petrov, L., Boy, J.: *Study of the Atmospheric Pressure Loading Signal in Very Long Baseline Interferometry Observations.* Journal of Geophysical Research, 109 (B03405), 2007

[18] Goddard Space Flight Center: http://lacerta.gsfc.nasa.gov/aplo_eph

[19] Schwerdt, M., Bräutigam, B., Bachmann, M., Döring, B., Schrank, D., Gonzalez, J.H.: *Final TerraSAR-X Calibration Results Based on Novel Efficient Methods.* IEEE Trans. on Geosci. and Remote Sens., Vol. 48, No. 2, 2010, pp. 677–689

[20] Fritz, T., Eineder, M.: *TerraSAR-X Ground Segment Basic Product Specification Document.* TX-GS-DD-3302, v1.5, 2008